Disclaimer

This note has not been internally reviewed by the DØ Collaboration. Results or plots contained in this note were only intended for internal documentation by the authors of the note and they are not approved as scientific results by either the authors or the DØ Collaboration. All approved scientific results of the DØ Collaboration have been published as internally reviewed Conference Notes or in peer reviewed journals.

Super-gravity Inspired SUSY Search in the Dielectron Channel

N.K. Mondal, V.S. Narasimham, H.C. Shankar

TIFR, Bombay

and

Kaushik De

University of Texas, Arlington

DØ NOTE # 2763

Abstract

The results from the Run 1A squark-gluino search at D0 in the jets and the missing E_t channel have already been published. With the accumulation of more luminosity in Run 1B, complementary searches in other channels have become more viable. This note summarizes the work done for the super-gravity motivated susy search in the di-electron channel. The results from the Monte Carlo studies and the analysis of the complete Run 1B data of integrated luminosity 90 pb^{-1} are presented.

I. INTRODUCTION

Supersymmetry is a space time symmetry linking fermions to bosons [1–5]. Supersymmetric extensions of the Standard Model envision a bosonic (fermionic) 'super-partner' for every standard model fermion (boson) and with the same internal quantum numbers. Although to date there has been no direct experimental evidence suggesting their validity, they have interesting theoretical and phenomenological properties which provide enough

motivation for their continued theoretical and experimental analyses.

II. SUPERSYMMETRIC MODELS

The simplest possibility is the minimal supersymmetric model (MSSM) which is a direct supersymmetrization of the Standard Model. The MSSM is *minimal* in that it contains a minimum number of new particles and interactions to be consistent with phenomenology. In this model, with the additional constraint of the baryon and lepton number conservation, it is possible to define a multiplicatively conserved quantum number called the R-parity which is +1 for the SM particles and -1 for their super-partners. A direct consequence of this is the fact that the lightest supersymmetric particle (LSP) is stable. The LSP is unlikely to be colored or electrically charged or else it would bind with nuclei and atoms to form heavy isotopes and would have been detected by now. Thus, the LSP, which is the end product of every supersymmetric particle decay, evades detection resulting in an overall energy-momentum imbalance.

The MSSM introduces just one partner (sparticle) for each SM particle. The gauge group is the SM gauge group SU(3) x SU(2) x U(1) and the corresponding spin 1 gauge bosons g, W, Z, γ have spin 1/2 gaugino partners $\tilde{g}$, $\tilde{W}, \tilde{Z}$, $\tilde{\gamma}$. The three generations of the spin 1/2 quarks q and the leptons l have the spin-0 squark and slepton partners $\tilde{q}$ and $\tilde{l}$. For a given fermion f, the left and right chiral states have distinct spartners $\tilde{f}_L$ and $\tilde{f}_R$. For anomaly cancellation, the single Higgs doublet is replaced by two doublets H_1 and H_2 that have the higgsino partners $\tilde{H}_1$ and $\tilde{H}_2$.

In principle, the supersymmetric particles with the same internal quantum numbers (spin, color and electric charge) can mix to form the mass eigenstates. such mixing between left and right handed sfermions (super partners of fermions) is proportional to the corresponding fermion mass and is usually small except for top squark unless the ratio of the vacuum expectation values of the two Higgs doublet ($\tan(\beta)$) is very large. The gluinos being the only color octet spin 1/2 particles does not have any mixing. However the mixing

among the electroweak gauginos and Higgsinos can be large. Such gaugino-Higgsino mixing results in two physical chargino mass eigenstates called $\tilde{W}_2^{\pm}$ and $\tilde{W}_1^{\pm}$ and four neutralino mass eigenstates called $\tilde{Z}_4$, $\tilde{Z}_3$,$\tilde{Z}_2$ and $\tilde{Z}_1$. For various theoretical and astrophysical reasons the lowest mass neutralino ($\tilde{Z}_1$) is assumed to be the LSP.

The MSSM requires more than 20 new parameters for its description which makes the experimental analysis very difficult. The number of new parameters can be reduced by making certain assumptions or, in otherwords, by choosing a *framework*. Once the framework is chosen, an attempt can be made to test the class of models described within it.

In the present analysis, we concentrate on the super-gravity inspired supersymmetric models [6–8]. The popularity of these models stem from the fact that the precision measurements of the gauge couplings at LEP are consistent with the simplest supersymmetric SU(5) grand-unification. In these models, there are only four new *soft* susy-breaking parameters (soft because these terms parametrize the susy breaking without effecting the the property of cancellation of quadratic divergences) which can be taken to be: a common SUSY-breaking scalar mass (m_0) for all scalars (squarks,sleptons, Higgses), a common mass for all gauginos ($m_{1/2}$), a common value for all trilinear couplings (A_0), and a common value for all bilinear couplings (B_0). The masses and couplings at the weak scale are obtained from the above unification scale parameters using the renormalization group techniques.

Another advantage of working within the sugra framework is that one can consistently combine the results from various searches (stop, wino-zino etc.) in different channels (trilepton, dilepton) as excluded regions on a single 2-dimensional m_0 - $m_{1/2}$ plot as opposed to having different plots for each analysis (as is the case while working within the usual MSSM). This becomes possible in the framework we have chosen because the correlations between different sparticle masses are taken care of as they are evolved down to the electro-weak scale from the common unification masses m_0 and $m_{1/2}$ at the GUT scale.

III. EXPERIMENTAL SEARCH

As mentioned earlier, the R-parity conservation implies that the LSP is a stable particle. It has other implications : 1) the sparticles must be produced in pairs and 2) heavy sparticles decay to lighter sparticles. For example, a squark will decay into a quark and the LSP ($\tilde{Z}_1$) . A gluino will decay into a quark, an antiquark and the LSP. Since the LSP does not interact, in these models, one is always assured of the presence of a substantial missing E_t.

Some of the early searches for squarks and gluons at CERN and also at Tevatron where one was probing the low mass region assumed such one step decay of squarks and gluinos into quark jets and LSPs. In these searches, one looked for energetic jets (due to final state quarks) and missing E_t (due to the undetected stable and neutral LSPs) as the canonical SUSY signature.

However, as the mass limits for the SUSY particles; specially for squarks and gluinos were pushed higher due to their non-observation, it was realised that squarks and gluinos may be relatively heavy and instead of decaying directly to the lowest mass SUSY particle, their decay may proceed through other heavier chargino and neutralino intermediate states as these states become kinematically accessible. Although recent searches by both D0 and CDF have taken such cascade decays into account, they are confined to the canonical jets and missing E_t channel and thus sensitive only to the hadronic decays of higher mass charginos and neutralinos to the LSPs [9–11].

A. Search in the Dielectron Channel

In addition to their hadronic decays, the charginos and higher mass neutralinos can also decay leptonically. In fact, in certain regions of the SUSY parameter space there can be substantial enhancement of their leptonic decay branching fractions. In such scenarios, the final state will consists of jets and several isolated leptons in association with missing E_t due to final state LSPs. Leptonic SUSY search using jets, isolated leptons and missing E_t

therefore compliment the canonical susy searchs which looked only for the jets and missing E_t and offer new ways of searching for SUSY particles. It is also possible to combine these two complimentary techniques in order to explore a much larger section of the SUSY parameter space.

With the collection of about 90 pb^{-1} of data in Run 1B and the availability of more elaborate susy event generators, a search in the leptonic channels has become more viable at DØ . The DØ detector is well suited with its good calorimetry and the eta coverage for electrons and jets for a search in the dielectron channel. In this analysis, one is interested in final states which have atleast two isolated, high E_t electrons, two jets and missing E_t.

IV. EVENT GENERATION:

A. Signal

As was discussed earlier, an interesting class of models is described by the four soft parameters (m_0, $m_{1/2}$, A_0, B_0). ISAJET version 7.13 [12] was used for the signal Monte Carlo event generation and the input parameters for this program are m_0, $m_{1/2}$, A_0 , $\tan(\beta)$ (which is the ratio of the vacuum expectation values of the two Higgs fields), $\mathrm{sgn}(\mu)$ (μ is the supersymmetric Higgsino mixing parameter) and m_t. This parameter set is equivalent to the set mentioned earlier because the constraint of the electro-weak symmetry breaking allows one to trade B_0 in favour of $\tan(\beta)$ and also to fix the magnitude of the μ parameter to get the Z boson mass. Of these, the values of four of the parameters A_0, $\tan(\beta)$, $\mathrm{sgn}(\mu)$, m_t are fixed[1] at 0, 2, -1 and 180 GeV respectively and the values for m_0 and $m_{1/2}$ are allowed to float on the 2-dimensional m_0-$m_{1/2}$ plane. This effectively reduces the number of free parameters to just two and the results can then be presented on the m_0-$m_{1/2}$ plane. The advantage of plotting the result in such a way is that the results from different searches

[1]at present efforts are underway to determine the effect of changing $\tan(\beta)$ and the $\mathrm{sgn}(\mu)$

(corresponding to different topologies) can be combined on a single plot. To choose the interesting values for m_0 and $m_{1/2}$, a first pass was made over various different values on this 2-d plane at the generator level to find out the region(s) which could be excluded. A subset of these points was taken and between 7,000 to 20,000 events were generated for each point. Events for more than 110 points have been generated so far. A reasonably fine 'mesh' is needed in the m_0-$m_{1/2}$ plane to be sensitive to the effects of the changing branching ratios to the dileptons. Since one is interested in the dielectron final states coming from all of the susy decays, the total cross section was generated which consisted of final states coming from all of the allowed susy processes incorporated in the generator. The dilepton events were streamed out by putting very loose generator level cuts for further processing through the detector/trigger simulation and the final event reconstruction. The generator level cuts required that there be atleast two leptons (electrons or muons) with $E_t > 3$ GeV and atleast two pjets with $E_t > 5$ GeV. These events were then processed through the showerlibrary, trigger simulator and D0RECO. The points where the events have been generated in the m_0-$m_{1/2}$ plane are shown in Fig. 1.

1. SUSY Cross Sections and Mass Spectrum

In Figs. 2 and 3 the cross-section (total) and the masses of the squarks, gluinos, $\tilde{W}_1$ and $\tilde{Z}_2$ as given by ISAJET are plotted as lego plots as a function of m_0 and $m_{1/2}$. It is seen that the cross section falls more steeply with $m_{1/2}$ than with m_0. The branching ratios to the dileptonic final states varies with m_0 and $m_{1/2}$ and the expected event yield at a given point in the m_0-$m_{1/2}$ plane for a given luminosity will depend on a convolution of these two effects. The squarks become heavier with increasing m_0 and $m_{1/2}$. The mass of gluinos depends mostly on $m_{1/2}$ and weakly on m_0 due to the radiative correction the gluino masses receive from the squarks. $\tilde{W}_1$ and $\tilde{Z}_2$ masses also depends mostly on $m_{1/2}$ becoming heavier with the increase of $m_{1/2}$.

B. Background

The principal *physics* background processes leading to events that mimic the signal final states are :

- $t\bar{t} \rightarrow$ ee
- WW $\rightarrow$ ee
- Z $\rightarrow$ ee
- Z $\rightarrow \tau\tau \rightarrow$ ee and
- QCD $\rightarrow$ ee (from $b\bar{b}, c\bar{c}$)

For the physics backgrounds, previously generated Monte Carlo events were used. The details of these events are given below:

Process	No. of events	Generator	Remark
$t\bar{t} \rightarrow$ ll (180 GeV)	2012	ISAJET 6.48	forced
WW $\rightarrow$ ee	2485	ISAJET 6.48	forced
Z $\rightarrow \tau\tau \rightarrow$ ll	1996	PYTHIA	forced, Z $P_t > 25GeV$
Z $\rightarrow$ ee	9970	ISAJET 6.48	forced
QCD $\rightarrow$ ee (from $b\bar{b}, c\bar{c}$)		ISAJET 6.48	(total σ)
	3288		pt range 40-60 GeV
	4956		pt range 60-80 GeV
	2695		pt range 80-100 GeV
	4417		pt range 100-130 GeV
	3348		pt range 130-160 GeV
	2922		pt range 160-200 GeV
	2100		pt range 200-240 GeV

Here, ll means e or μ. For top, the decays to dileptons through τ are also included.

In addition, there is also the instrumental background coming from some events in which a jet is mis-identified as an electron. In such events, there is one real electron and atleast three jets out of which one is misidentified and is counted as an electron. This background was estimated using the $w + jets$ data sample. More details on the background estimation are given in section 5.

V. MONTE CARLO AND DATA ANALYSIS

The kinematic cuts were designed after a study of the kinematics of the susy events and the background processes. These are such that atleast a few signal events remained for a reasonable signal to background ratio.

A. Event Selection

1. Electron Definition

The parameters used in defining an electron for this analysis are

1. *EM fraction* (f_{EM})
2. *Cluster Shape* (χ^2)
3. *Trackmatch Significance (S)* and
4. *Isolation* (f_{iso})

The D0RECO makes a cut only on f_{EM} ($f_{EM} > 0.9$) in identifying an object as an electron. The other parameters were used to achive more rejection against the backgrounds while maintaining a reasonable electron identification efficiency for electrons coming from the susy decays.

The electron is defined to be an object satisfying the following requirements in addition to the cut on f_{EM}:

$f_{iso} < 0.1$, $\chi^2 < 100$, S < 5.0

The efficiencies for these cuts have been determined from the $Z- > ee$ data to be 88.8±0.9 (%) in CC and 72.3±2.3 (%) in EC. These efficiencies have been determined for electrons from the $Z- > ee$ data with $E_t > 25$ GeV [13]. Since one cannot use these efficiencies for lower E_t electrons directly, a parametrization of the efficiency as a function of electron E_t obtained from plate level monte carlo electrons overlaid with real minimum bias data has been used to estimate the low E_t efficiencies. A sample generated at $\eta = 0.4$ was used to determine the efficiencies for CC electrons, while another sample at $\eta = 2.0$ was used for the EC electrons [14].

The efficiencies for track finding in CC and EC are 86.7±1.4 (%) and 86.1±1.8 (%) respectively [13]. These efficiencies have been determined using the $Z- > ee$ data and are assumed to be independent of the track P_T.

2. Offline Cuts

Two different sets of cuts exploiting the signal and background characteristics have been used to optimize the signal to background ratio. The two differ only w. r. t. the invariant mass of the electron pair. In the first, Analysis I, we use the standard Z-mass cut to supress the Z background. As we will see later, this set is quite effective for all the backgrounds except the top, as the top dielectron events are quite similar to the susy signal events. The second set, Analysis II makes use of the unique characteristic of the signal dielectron invariant mass spectrum to supress the top background significantly. In the present note, we mainly concentrate on analysis I. Results from analysis II will be discussed seperately.

The offline cuts are the following:

– atleast two electrons with an $E_t > 15$ GeV within an $| \eta | < 2.5$

- atleast two jets with an $E_t > 20$ GeV within an $\mid \eta \mid < 2.5$ satisfying jet quality cuts

- missing $E_t > 25$ GeV for all events

- Invariant mass cut:

  o $\mid inv\_mass(e,e) - m_z \mid > 12$ GeV or $E_t > 40$ (Present analysis).

  o $inv\_mass < 80$ GeV (Analysis II).

3. Trigger cuts

In addition to the electron id cuts and the offline kinematic and geometric cuts described above, the following Level 2 trigger have been used for event selection.

o ELE_JET_HIGH

L2EM(1,15) + L2JET(2,10) + MS(14) and

For this trigger, atleast one 15 GeV electromagnetic cluster, two 10 GeV jets and a minimum missing E_t of 14 GeV are required at L2. Since the offline cuts are much harder than the trigger thresholds, between 93%-100% of the events passing the offline cuts also satisfy the trigger requirement.

B. Effect of the Cuts on the Signal and the Background

In this section, the motivation for the above mentioned cuts is discussed in the order in which the cuts are applied. In the following figures, for the signal, a typical point has been chosen on the m_0-$m_{1/2}$ for which $m_0 = 180$ GeV and $m_{1/2} = 90$ GeV.

Electron Cuts.

In Fig. 4, the electron E_t and isolation distributions for the signal and the QCD background coming from $b\bar{b}, c\bar{c}$ are shown along with the cuts. Figs. (a) and (b) are for the trailing electron and (c) and (d) are for the leading electron. These cuts predominatly suppress the QCD background as these events have low E_t, non-isolated electrons. The signal events on the other hand have a harder electron E_t spectrum and do not have as much accompanying energy. A significant number of events from top, WW and Z pass these cuts. Invariant Mass Cut.

For Analysis I, an event is rejected if the invariant mass of the electron pair reconstructs the Z-mass to within 12 GeV and if the missing E_t is less than 40 GeV. Figs. 5 (a) and (b) show the missing E_t vs. the invariant mass for the signal and the Z events. The Z to ee events have no real missing E_t and the observed missing E_t spectrum is due to the detector effects. Furthermore, this spurious missing E_t has a cut off at about 40 GeV and so an event is considered if its missing E_t is greater than 40 GeV even if it lies inside the Z-window.

The invariant mass distribution for the top and the WW are quite wide and have a long tail. The Z-mass cut is not so effective against these two backgrounds as it just takes off a small slice of events at the Z-mass.

Analysis II uses a different invariant mass cut which is effective against all the three background processes: top, Z and WW. Figs. 5 (c) and (d) show the invariant mass distributions for the signal and the top events. The invariant mass cut at 80 GeV is shown by the down arrows. It is a characteristic feature of the susy events that the invariant mass is clustered at the lower end of the spectrum. This is due to the fact that in a considerable region of the parameter space, the electrons in the susy events come predominantly from the second lightest neutralino $\tilde{Z}_2$ which then almost always decays into two oppositely charged same flavor leptons and the LSP ($\tilde{Z}_1$). The width of the invariant mass clustering is determined by the difference in the masses of $\tilde{Z}_1$ and $\tilde{Z}_2$ modulo the phase space. This fact has been exploited in making this cut and the Fig. 5 (d) shows how this cut suppresses the top

background quite significantly. It is also to be noted that this cut effectively suppresses the Z background as well.

The Missing E_t Cut.

At this stage, much of the background is from Z $\rightarrow \tau\tau$, WW $\rightarrow$ ee and Drell-Yan events. The surviving Z $\rightarrow$ ee events are due to mis-measured electrons. However, these events are not expected to have much missing E_t. Figs. 6 (a), (b) and (c) show the missing E_t distributions for the signal, WW and Z $\rightarrow \tau\tau$. Fig. (c) makes the efficacy of this cut very clear with regard to supressing the Z $\rightarrow \tau\tau$ events, while still maintaining good efficiency for the signal.

The surviving physics background contribution now comes mainly from the WW events for which the jet cut is designed.

The Jet Cut.

The WW events are similar to top and signal in the electron E_t, invariant mass and missing E_t but they are not expected to have two high et jets. The susy events on the other hand, have a rich jet spectrum and a requirement of two jets above a 20 GeV threshold gives a good efficiency for the signal. This becomes evident from Fig. 7 (a),(b) and (c) where the jet multiplicity distribution for jets with $E_t > 20$ GeV is shown for the signal, WW and Z $\rightarrow \tau\tau$ respectively. This cut is effective against the WW and also against the other residual backgrounds (including the fakes).

C. Signal Efficiencies and the Expected Event Yield

This section gives the estimated signal event yields and summarizes the contributions from all the background channels for a luminosity of 90 pb^{-1}.

Tables I summarize the over all efficiency*b.r.(%) and the expected event yields for some of the monte carlo points in the m_0-$m_{1/2}$ plane.

TABLE I

m_0	$m_{1/2}$	$\epsilon\times$B.R.(%)	$< N >$	m_0	$m_{1/2}$	$\epsilon\times$B.R.(%)	$< N >$
0	85	$0.08\pm0.01^{+0.00}_{-0.00}$	8.26 ± 1.63	0	90	$0.11\pm0.01^{+0.00}_{-0.00}$	3.40 ± 0.56
0	95	$0.21\pm0.02^{+0.00}_{-0.01}$	1.79 ± 0.21	10	85	$0.06\pm0.01^{+0.00}_{-0.00}$	5.12 ± 1.23
10	90	$0.10\pm0.01^{+0.00}_{-0.00}$	2.06 ± 0.35	20	85	$0.13\pm0.02^{+0.00}_{-0.00}$	5.60 ± 0.88
20	90	$0.24\pm0.03^{+0.00}_{-0.00}$	2.64 ± 0.39	30	70	$0.06\pm0.01^{+0.00}_{-0.00}$	12.04 ± 2.45
30	75	$0.06\pm0.01^{+0.00}_{-0.00}$	6.20 ± 1.28	30	85	$0.23\pm0.02^{+0.00}_{-0.00}$	2.96 ± 0.32
40	70	$0.09\pm0.01^{+0.00}_{-0.00}$	5.88 ± 0.96	40	80	$0.16\pm0.02^{+0.00}_{-0.00}$	2.38 ± 0.34
50	60	$0.16\pm0.02^{+0.00}_{-0.00}$	11.02 ± 1.45	50	70	$0.18\pm0.02^{+0.00}_{-0.00}$	4.71 ± 0.62
50	85	$0.21\pm0.02^{+0.00}_{-0.00}$	2.04 ± 0.26	60	55	$0.10\pm0.01^{+0.00}_{-0.00}$	7.89 ± 1.21
60	65	$0.08\pm0.01^{+0.00}_{-0.00}$	2.93 ± 0.50	70	40	$0.73\pm0.04^{+0.00}_{-0.01}$	224.89 ± 14.52
70	50	$0.02\pm0.00^{+0.00}_{-0.00}$	2.55 ± 0.87	80	80	$0.69\pm0.04^{+0.01}_{-0.00}$	7.04 ± 0.49
80	85	$0.77\pm0.05^{+0.00}_{-0.01}$	5.71 ± 0.40	80	90	$0.55\pm0.05^{+0.01}_{-0.01}$	3.13 ± 0.30
90	70	$0.73\pm0.06^{+0.00}_{-0.01}$	13.85 ± 1.15	90	75	$0.97\pm0.08^{+0.01}_{-0.02}$	13.02 ± 1.14
100	85	$1.06\pm0.07^{+0.02}_{-0.01}$	7.10 ± 0.51	120	85	$1.23\pm0.08^{+0.00}_{-0.02}$	7.21 ± 0.48
120	90	$1.16\pm0.08^{+0.01}_{-0.01}$	5.34 ± 0.38	130	80	$1.43\pm0.09^{+0.01}_{-0.01}$	10.63 ± 0.66
130	87	$1.26\pm0.08^{+0.01}_{-0.02}$	6.20 ± 0.40	140	60	$1.74\pm0.10^{+0.00}_{-0.01}$	43.66 ± 2.53
140	90	$1.42\pm0.09^{+0.00}_{-0.03}$	5.63 ± 0.37	150	80	$1.52\pm0.09^{+0.02}_{-0.01}$	9.97 ± 0.63
150	85	$1.20\pm0.06^{+0.01}_{-0.00}$	5.91 ± 0.33	150	90	$1.16\pm0.08^{+0.01}_{-0.00}$	4.40 ± 0.31
170	80	$1.45\pm0.09^{+0.01}_{-0.01}$	8.58 ± 0.55	170	85	$1.26\pm0.10^{+0.01}_{-0.01}$	5.66 ± 0.44
180	55	$0.71\pm0.06^{+0.01}_{-0.00}$	19.76 ± 1.65	180	70	$1.49\pm0.09^{+0.01}_{-0.01}$	14.73 ± 0.93
180	75	$1.39\pm0.10^{+0.01}_{-0.01}$	10.34 ± 0.79	200	65	$0.66\pm0.05^{+0.02}_{-0.01}$	8.12 ± 0.71

TABLE I (contd.)

m_0	$m_{1/2}$	$\epsilon \times$B.R.(%)	$< N >$	m_0	$m_{1/2}$	$\epsilon \times$B.R.(%)	$< N >$
200	100	$0.93 \pm 0.07^{+0.02}_{-0.00}$	1.82 ± 0.14	220	50	$0.41 \pm 0.03^{+0.02}_{-0.01}$	15.14 ± 1.45
220	90	$0.91 \pm 0.06^{+0.01}_{-0.01}$	2.74 ± 0.18	250	45	$0.10 \pm 0.01^{+0.00}_{-0.00}$	14.41 ± 2.48
250	60	$0.33 \pm 0.03^{+0.00}_{-0.00}$	5.09 ± 0.52	265	65	$0.17 \pm 0.02^{+0.00}_{-0.00}$	1.85 ± 0.22
265	85	$0.35 \pm 0.03^{+0.00}_{-0.00}$	1.23 ± 0.11	280	70	$0.33 \pm 0.03^{+0.01}_{-0.00}$	2.52 ± 0.25
300	50	$0.19 \pm 0.02^{+0.00}_{-0.00}$	7.94 ± 1.06	300	60	$0.22 \pm 0.03^{+0.00}_{-0.00}$	3.42 ± 0.46
320	35	$0.01 \pm 0.00^{+0.00}_{-0.00}$	12.74 ± 4.82	340	50	$0.13 \pm 0.01^{+0.00}_{-0.00}$	6.66 ± 0.87
350	55	$0.18 \pm 0.02^{+0.00}_{-0.00}$	4.40 ± 0.51	370	50	$0.10 \pm 0.01^{+0.00}_{-0.00}$	6.21 ± 1.01
370	70	$0.15 \pm 0.02^{+0.00}_{-0.01}$	1.25 ± 0.17	380	55	$0.12 \pm 0.01^{+0.00}_{-0.00}$	3.24 ± 0.42
390	50	$0.06 \pm 0.01^{+0.00}_{-0.00}$	4.30 ± 0.91	390	70	$0.12 \pm 0.01^{+0.01}_{-0.00}$	1.00 ± 0.16
400	40	$0.02 \pm 0.01^{+0.00}_{-0.00}$	9.67 ± 4.01	400	55	$0.10 \pm 0.01^{+0.00}_{-0.00}$	2.87 ± 0.39
400	70	$0.10 \pm 0.02^{+0.01}_{-0.01}$	0.88 ± 0.16	420	55	$0.14 \pm 0.01^{+0.00}_{-0.01}$	4.03 ± 0.48

1. Origin of the Events Passing all Off-line Cuts

As reported earlier, the Monte Carlo signal event generation consisted of generating the total susy cross-section. This means that the original sample set consists of events coming from all allowed susy processes *viz.*, gluino-gluino, squark-squark, squark-gluino, wino-zino, gluino/squark-wino/zino, slepton/sneutrino-slepton/sneutrino etc. It is of interest to see what fraction of the events passing all off-line cuts populate what class of processes. To illustrate this, two cases have been considered; one in which $m_{1/2}$ has been fixed at 60 and m_0 is allowed to vary and the other in which $m_{1/2}$ is fixed at 90 and m_0 is varied across a wide range. Tables *II* and *III* show the percentage of events that pass the offline cuts belonging to these different classes. It can be seen from these two tables that except at very high m_0, events with gluinos and quarks in the initial state dominantly pass our offline cuts.

TABLE II ($m_{1/2} = 60$)

m_0	$\tilde{s} - \tilde{s}$	$\tilde{g} - \tilde{g}$	$\tilde{s} - \tilde{g}$	total $\tilde{s}\tilde{g}$	$\tilde{W}_i - \tilde{Z}_i$	$\tilde{s}/\tilde{g} - \tilde{W}_i/\tilde{Z}_i$	$\tilde{l}/\tilde{\nu} - \tilde{l}/\tilde{\nu}$
100	16.36	24.36	48.73	89.45	3.27	6.91	0.36
120	26.33	21.67	41.67	89.67	1.00	9.00	0.33
140	26.32	18.27	44.89	89.47	1.24	9.29	0.00
250	9.57	45.74	28.72	84.04	6.38	9.57	0.00
300	0.00	76.19	14.29	90.48	4.76	4.76	0.00
350	0.00	55.56	7.41	62.96	18.52	18.52	0.00

TABLE III ($m_{1/2} = 90$)

m_0	$\tilde{s} - \tilde{s}$	$\tilde{g} - \tilde{g}$	$\tilde{s} - \tilde{g}$	total $\tilde{s}\tilde{g}$	$\tilde{W}_i - \tilde{Z}_i$	$\tilde{s}/\tilde{g} - \tilde{W}_i/\tilde{Z}_i$	$\tilde{l}/\tilde{\nu} - \tilde{l}/\tilde{\nu}$
20	64.44	0.00	8.89	73.33	8.89	13.33	4.44
50	47.73	4.55	18.18	70.45	11.36	13.64	4.55
80	49.48	3.09	22.68	75.26	6.19	15.46	3.09
100	30.12	6.95	32.05	69.11	8.88	20.46	1.54
120	30.00	11.43	30.48	71.90	6.19	20.95	0.95
140	21.95	16.26	36.99	75.20	6.10	16.67	2.03
150	22.73	18.18	25.76	66.67	7.58	21.21	4.55
180	27.83	14.68	34.25	76.76	7.95	14.68	0.61
220	27.46	17.21	30.33	75.00	9.43	15.57	0.00
250	21.58	12.95	21.58	56.12	25.18	18.71	0.00
300	22.45	24.49	20.41	67.35	12.24	20.41	0.00
350	10.00	30.00	3.33	43.33	30.00	26.67	0.00

D. Background Estimates

For estimating contributions from various background sources, previously generated Monte Carlo event samples have been used. However, these events are used only to estimate the effect of various offline cuts. i.e. to estimate the efficiencies. Experimentally measured cross sections are then folded in to predict the number of background events from various sources.

1. Physics Backgrounds

For the top, the total measured cross-section of 4.69 ± 1.62 pb (D0) has been used [15]. Further, since the final states contain only e's or μ's (which may come directly or through τ decays), the effective cross section is obtained by multiplying the total cross-section with the relevant branching ratio, which in the present case is 6.85%. This gives an effective cross-section for top -> ll as 0.32 ± 0.11 pb.

For the Z -> ee process, the measured Z partial cross section for di-electrons, 230 ± 12 pb has been used [16].

In addition,for the Z to $\tau\tau$ case, the same cross-section has been assumed for Z going to $\tau\tau$ as it is for the Z -> ee process. The total branching ratio for $\tau\tau - - > ll$ is 12.67%. This gives an effective cross-section for $Z - - > \tau\tau - - > ll$ as 28.63 ± 1.26 pb. Also, since no events from the sample of Z $p_t < 25$ GeV, pass our cuts, we put a p_t of 25 GeV on the Z p_t to increase statistics at the generator level. According to CDF and D0 measurements only 13% of the total cross section [17] is above $p_t(Z) > 25$ GeV. In addition, this number has an error of 20 %. This gives the final effective cross section for $Z(p_t > 25GeV) - - > \tau\tau - - > ll$ as 3.78 ± 0.76 pb.

For the WW -> ee case, the WW production cross-section has been taken to be 10 pb which has then been multiplied by the branching ratio for WW->ee (1.23 %) to get the total effective cross-section for WW->ee as 0.123 pb.

2. Instrumental Background

The instrumental background (fakes) arises from the misidentification of jets as electrons. To get an estimate of this contribution, an $w + jets$ data sample was used. One first selects all the events in which there was atleast one electron and three jets satisfying the electron and jet cuts respectively. These events were also required to pass the missing E_t cut. Such events would then mimic the signal if one of the three jets were to be mis-identified as an electron. To get the estimate due to such fake events, the number of jets with $E_t > 20$ GeV was counted separately in CC and EC and added up. Then, using the fake probability numbers for a jet to fluctuate into an electron, an estimate was obtained. The Run 1b fake probabilities in CC and EC are given below:

(2. 74±0. 16) x 10E-4 (CC) and (3. 88±0. 41) x 10E-4 (EC)

3. Estimation of error

We have considered the following major sources of uncertainties while estimating the background contribution from various channel.

(a) Statistical error due to the finite size of the Monte Carlo sample used.

(b) Systematic error due to the jet energy scale uncertainty. We estimate this error by analyzing the Monte Carlo events with nominal, high and low CAFIX corrections and taking the difference as the error due to energy scale uncertainty.

(c) Since for most of the background channels, we have used experimentally measured cross sections, we also propagated the error in cross section measurement as a component of the systematic error.

Finally we have considered the luminosity error seperately while estimating the SUSY cross section limits.

4. Background Summary

Table IV, gives the break up of the various background contributions with the statistical and systematic errors. The first term is the statistical error. It also includes the error in the electron ID efficiency. All other sources of errors described above i.e. error due to energy scale uncertainty and error in cross section are included in the second term.

Table IV

Background Process	Expected Contribution to 90 pb^{-1}
$t\bar{t} \rightarrow$ ee (180 GeV)	1.165±0.050 ± 0.413
WW $\rightarrow$ ee	0.037±0.007 ± 0.002
Z $\rightarrow \tau\tau \rightarrow$ ee	0.241±0.028 ± 0.072
Z $\rightarrow$ ee	0.952±0.646 ± 1.001
QCD $\rightarrow$ ee (from $b\bar{b}, c\bar{c}$)	0.077*
fakes	0.436±0.026
Total	2.908±0.648 ± 1.085

* for these, since no events survived all the cuts, a 90% C.L. upperbound is given.

E. Effect of Cuts on the Run 1b Data

With the electron-id criteria and the offline and trigger requirements mentioned earlier, about 90 pb^{-1} of the 1B data was analysed and two events were found to survive all the cuts. The effect of the cuts on the 1b data are shown in Table VI and the details of the two events that passed the cuts are given in Table VII.

Table V

Cut	No. of events
Passed Trigger requirement	117191
Electron Quality Cuts	369
Electron Et/Eta Cuts	318
Z-mass Cut	104
Missing Et Cut	46
Jet Cuts	2
Expected Background	2.9±1.26

Table VI

Run No.	Event No.	Object	E_t(Gev)	η	ϕ (rad)
84634	15628	Electron 1	26.1	-1.08	2.80
		Electron 2	22.0	-1.72	6.12
		Jet 1	35.7	-0.75	5.35
		Jet 2	21.9	-0.80	1.40
		Missing Et	27.4		
		Inv. Mass	50.3		
88295	30317	Electron 1	50.5	0.33	1.52
		Electron 2	22.6	-1.49	1.90
		Jet 1	46.8	-0.72	4.04
		Jet 2	27.3	-0.92	4.84
		Missing Et	42.0		
		Inv. Mass	71.6		

VI. CROSS SECTION LIMITS AND THE EXCLUDED REGION

Since no excess of events is observed above the estimated background from the known Standard Model sources in the 90 pb^{-1} Run 1B data set, the parameter/mass region that is excluded by this analysis in the m_0-$m_{1/2}$ plane at 95% C.L. are determined in this section.

With the known values for the signal efficiencies at various points in the 2-d parameter space, the total luminosity of the data used, expected background contributions and the associated uncertainties in these quantities, the cross section limits were calculated [18] at the 95% confidence level for the points where events were generated in the m_0-$m_{1/2}$ plane. For the intermediate points, linear interpolation was used to calculate the expected total susy cross-sections and the cross-section limits.

The excluded region in the m_0-$m_{1/2}$ plane was found by comparing these two numbers i.e., a point was excluded whenever the theory cross section was found to be greater than the cross section limit at that point. The region, excluded at 95% C.L., is shown in Fig. 8. Here, (a) is the region that is excluded by theory and (b) is the region which is allowed theoretically but where the LSP is an sneutrino instead of the lightest neutralino. The dip in the contour around $m_0 = 70 - 80$ is the region where the sneutrinos became lighter than the $\tilde{Z}_2$. As a result, in this region of the parameter space, $\tilde{Z}_2$ dominantly decays into Z_1 and neutrinos through the sneutrino propagator thus reducing the branching ratio to dielectron final state substantially. As one moves to lower values of m_0, in addition to sneutrinos, the selctrons also become lighter than the $\tilde{Z}_2$ thus increasing the branching fraction to di-electrons again. The equivalent contour for the excluded region in the squark-gluino plane is shown in Fig. 9 where the squark mass is assumed to be the average of the squark masses of the first two generations. In the model under investigation, the gluino cannot be much heavier than the squarks. Due to this, the reach is confined to regions where the gluino mass is not too much heavier than the squark masses.

VII. RESULTS AND CONCLUSIONS AND FUTURE PLANS

From the present analysis, it is clear that no excess of events is observed above the number predicted by the Standard Model. Using this information and the Monte Carlo study of the signal at various points in the m_0-$m_{1/2}$ plane, this result is interpreted as an excluded region at the 95% confidence level on the same.

REFERENCES

[1] D. Volkov and V. Akulov. *Phys. Lett.*, 46B:109, 1973.

[2] T.Golfand and E. Likhtman. *JETP Lett.*, 13:323, 1971.

[3] P. Fayet and S. Ferrara. *Phys. Rep.*, 32:249, 1977.

[4] H. P. Nilles. *Phys. Rep.*, 110:1, 1984.

[5] H. E. Haber and G. L. Kane. *Phys. Rep.*, 117:75, 1985.

[6] S. Ferrara R. Barbieri and C. Savoy. *Phys. Lett.*, 119B:343, 1982.

[7] S. Deser and B. Zumino. *Phys. Lett.*, 62B:335, 1976.

[8] P. van Nieuwenhuizen. *Phys. Rep.*, 68:189, 1981.

[9] F. Abe et al. *Phys. Rev. Lett.*, 69:3439, 1992.

[10] S. Abachi et al. *Phys. Rev. Lett.*, 77:618, 1995.

[11] J.Hauser. In *Proc.* 10^{th} *Topical Worshop on Proton-Antiproton Collider Physics*, Fermilab, USA, May 1995.

[12] H. Baer, F. E. Paige, S. Protopopescu and X. Tata. Technical Report FSU-HEP-930329, UH-511-764-93, 1993.

[13] S.Chopra, U.Heintz, M.Narain. Technical Report D0note 2351, 1995.

[14] D. Norman. *Priv. Comm.*, 1995.

[15] Q. Li-Demarteau. *Aspen Winter Physics Conference , Aspen, Colorado* , TOBS, 1996.

[16] A. Spadafora. *Proc. of 10th Topical Workshop on* $p\bar{p}$ *collider Physics.*, page 382, 1995.

[17] F. Abe et. al. *Phys. Rev. Lett.*, TOBS, 1995.

[18] Marc Paterno et. al. Technical Report D0note 2775, 1995.

FIGURES

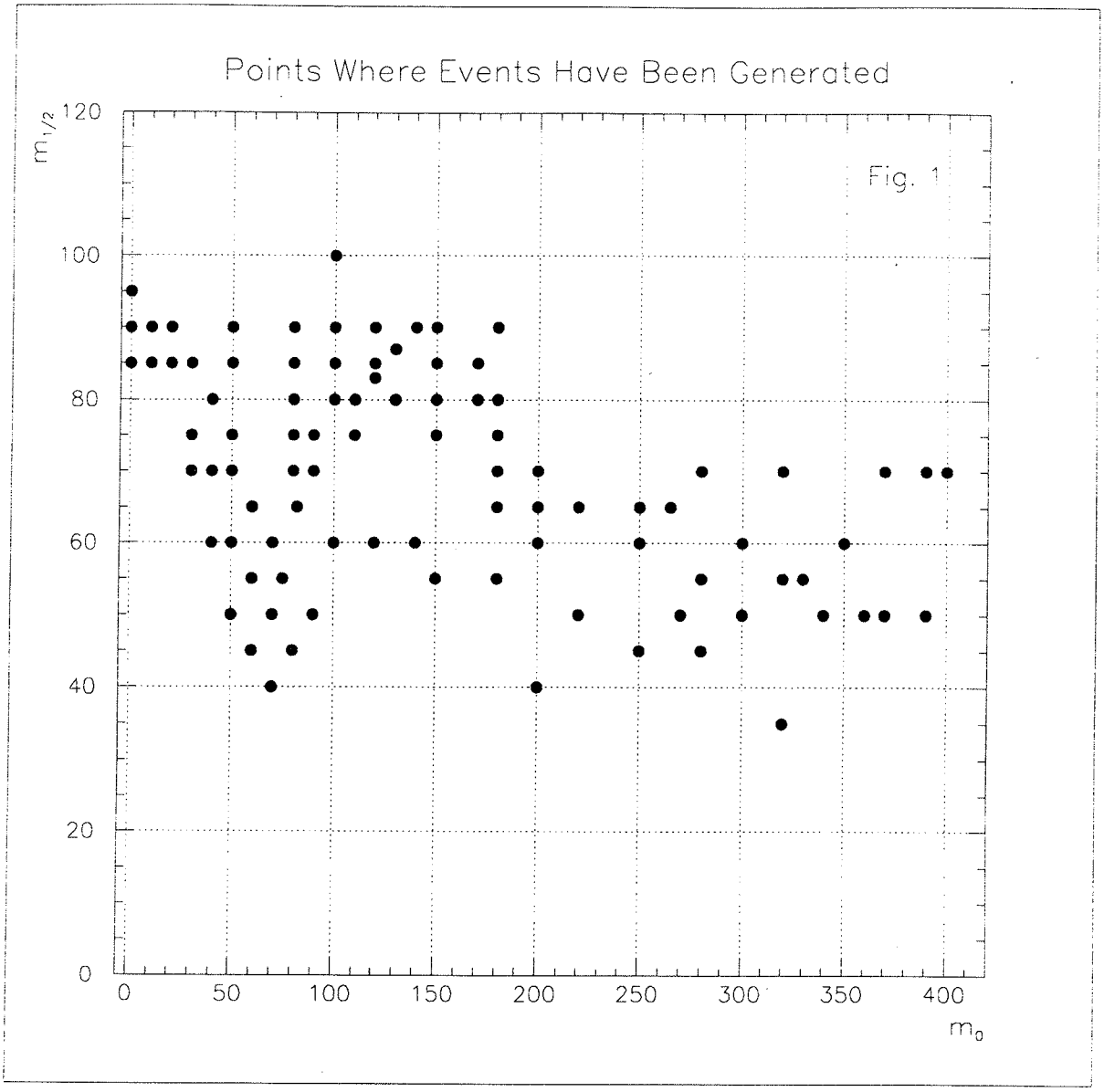

FIG. 1. Region Covered in the $m_0 - m_{1/2}$ Plane.

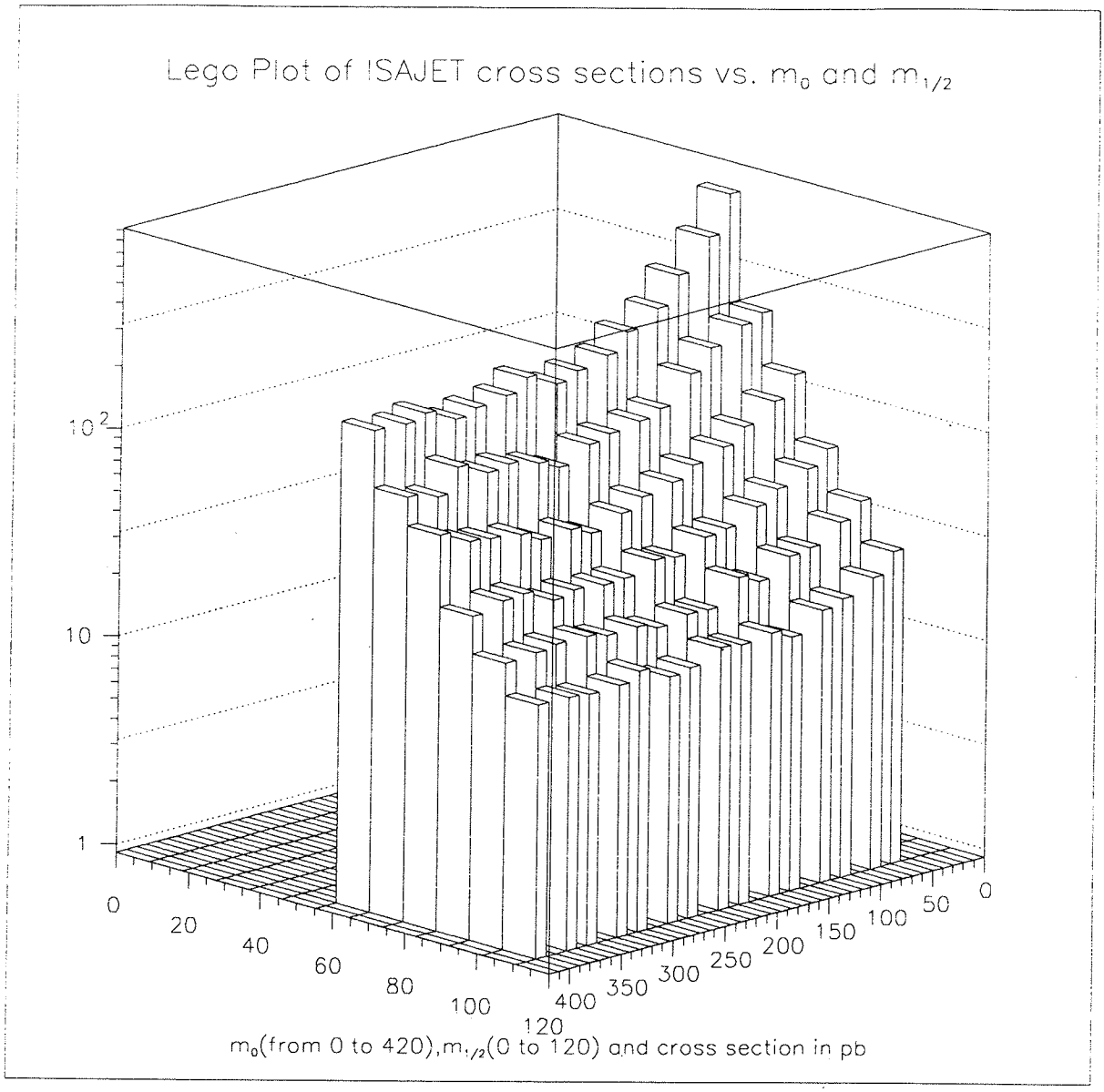

FIG. 2. ISAJET SUSY Cross-sections

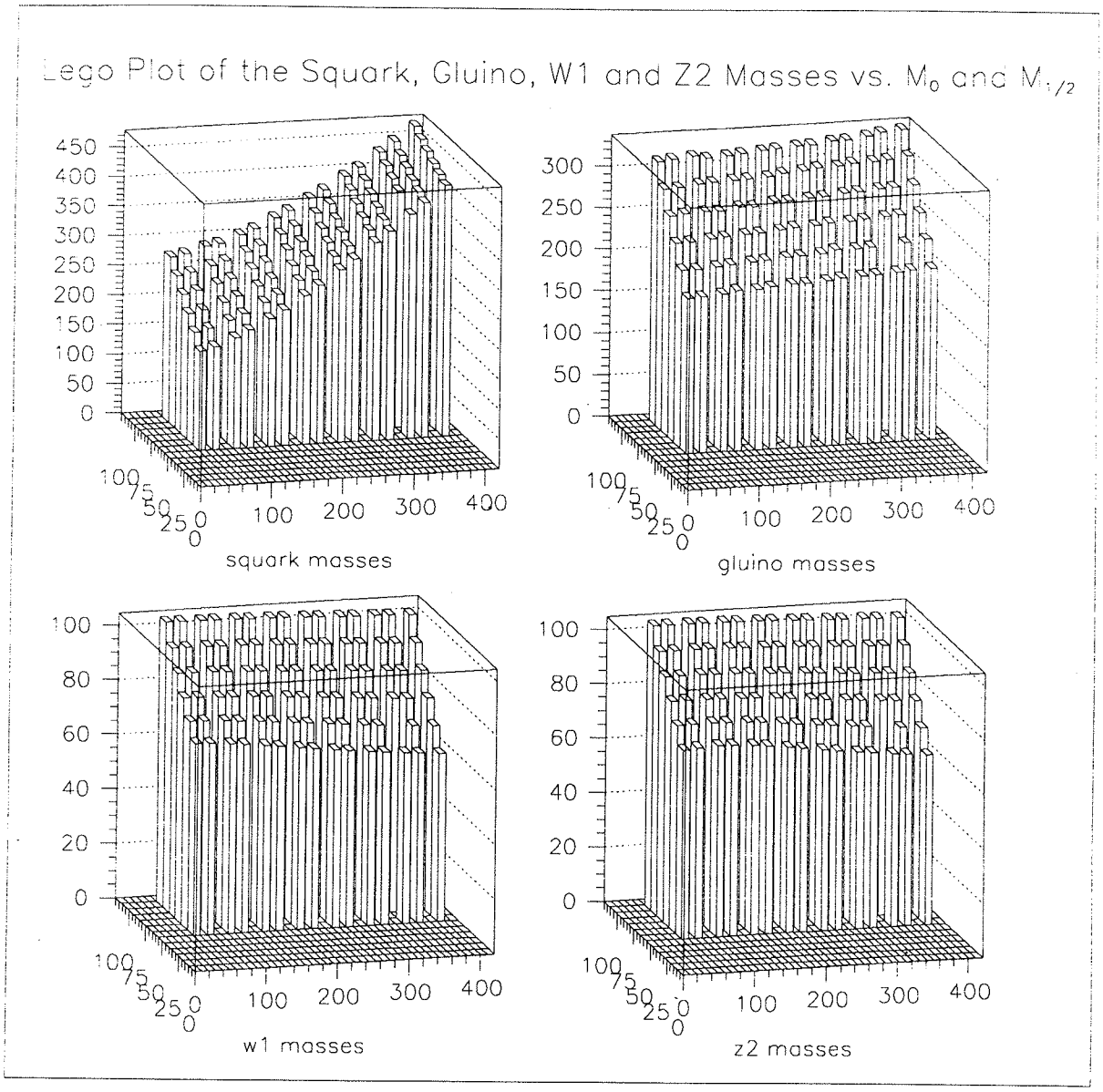

FIG. 3. ISAJET SUSY Mass Spectrum.

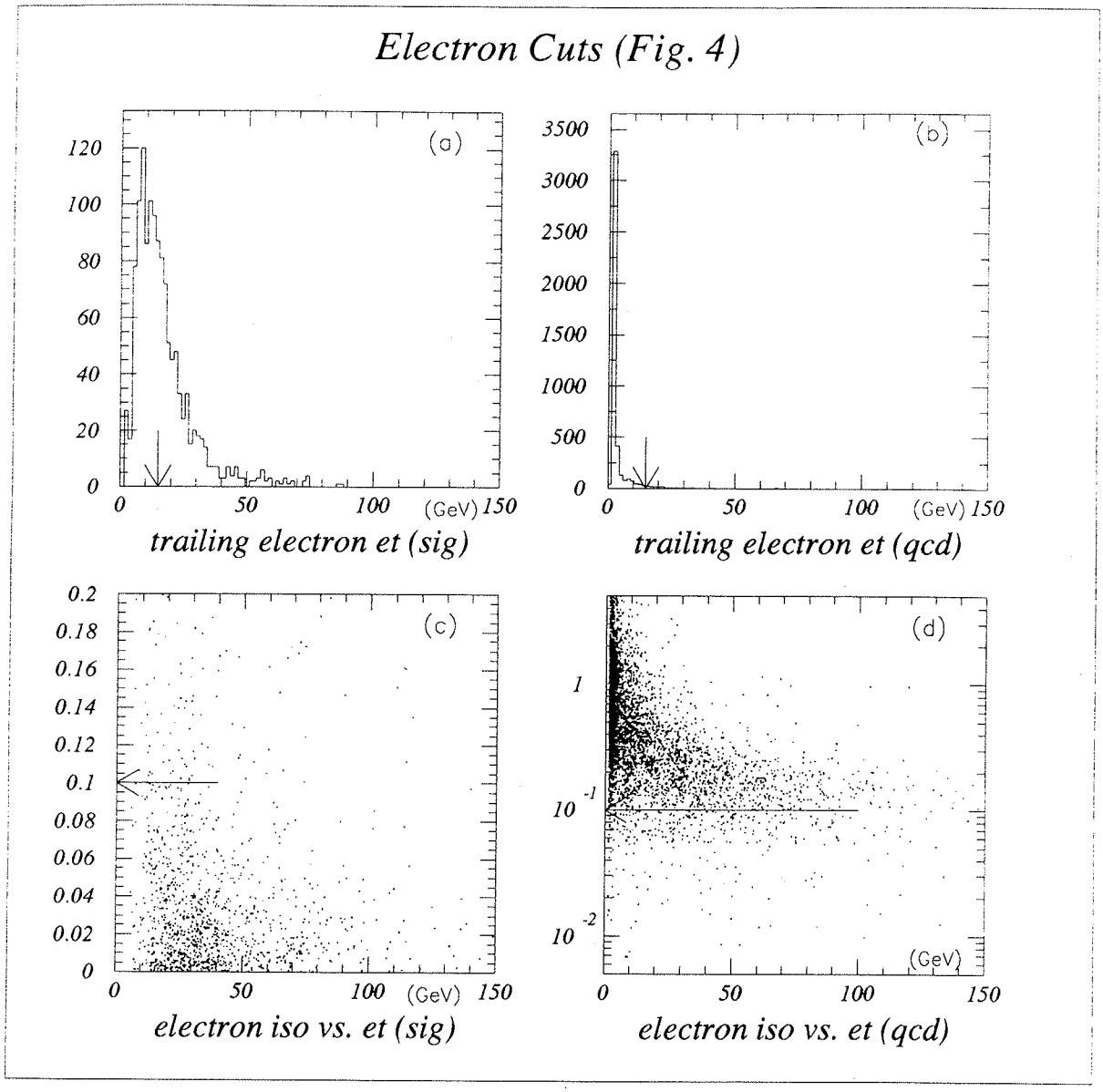
Electron Cuts (Fig. 4)
(a)
120
100
80
60
40
20
0
0
50
100
(GeV)
150
trailing electron et (sig)
(b)
3500
3000
2500
2000
1500
1000
500
0
0
50
100
(GeV)
150
trailing electron et (qcd)
(c)
0.2
0.18
0.16
0.14
0.12
0.1
0.08
0.06
0.04
0.02
0
0
50
100
(GeV)
150
electron iso vs. et (sig)
(d)
1
10 -1
10 -2
0
50
100
150
(GeV)
electron iso vs. et (qcd)

FIG. 4.

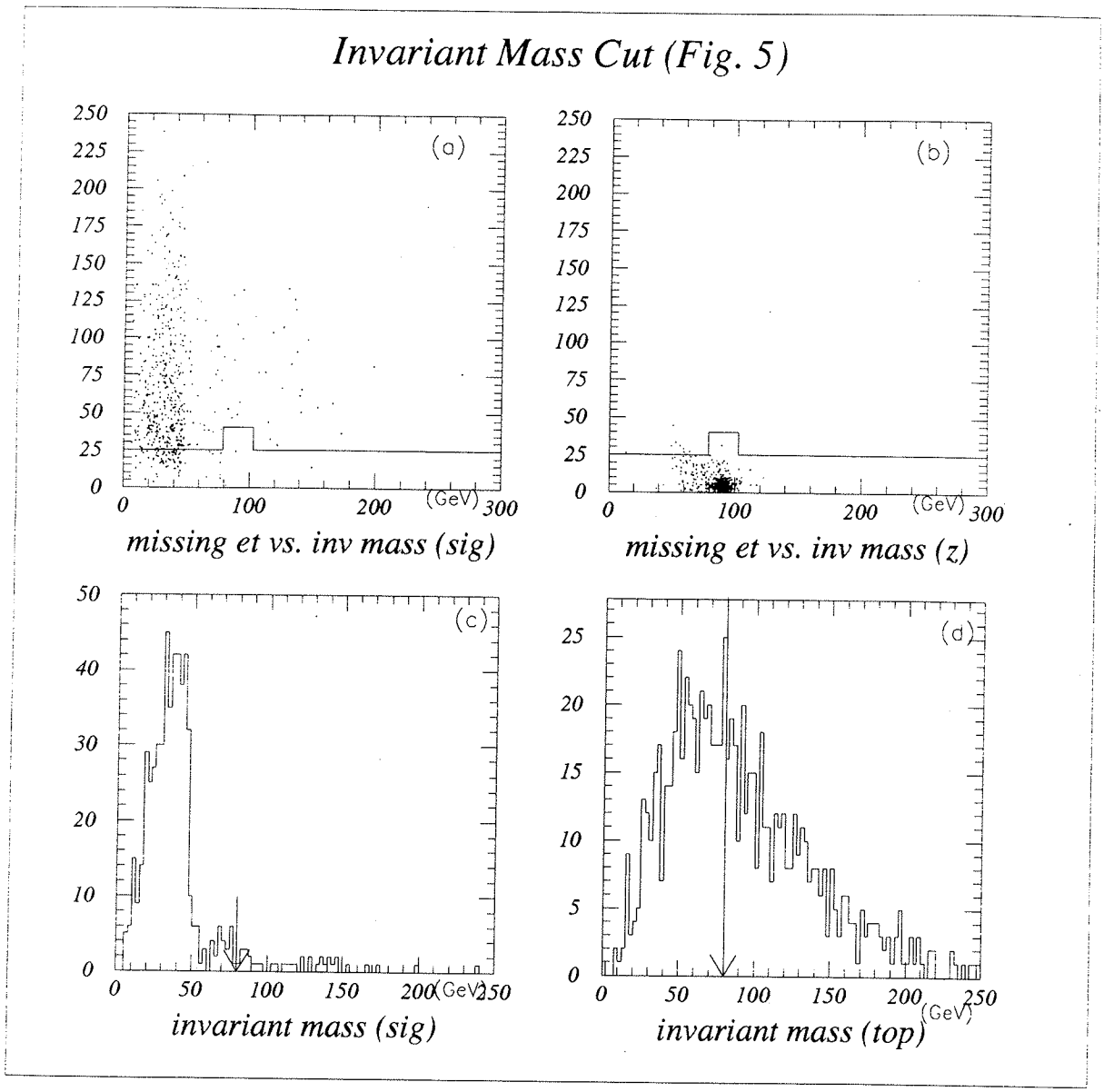
Invariant Mass Cut (Fig. 5)
(a)
(b)
(c)
(d)
(GeV)
missing et vs. inv mass (sig)
missing et vs. inv mass (z)
invariant mass (sig)
invariant mass (top)

FIG. 5.

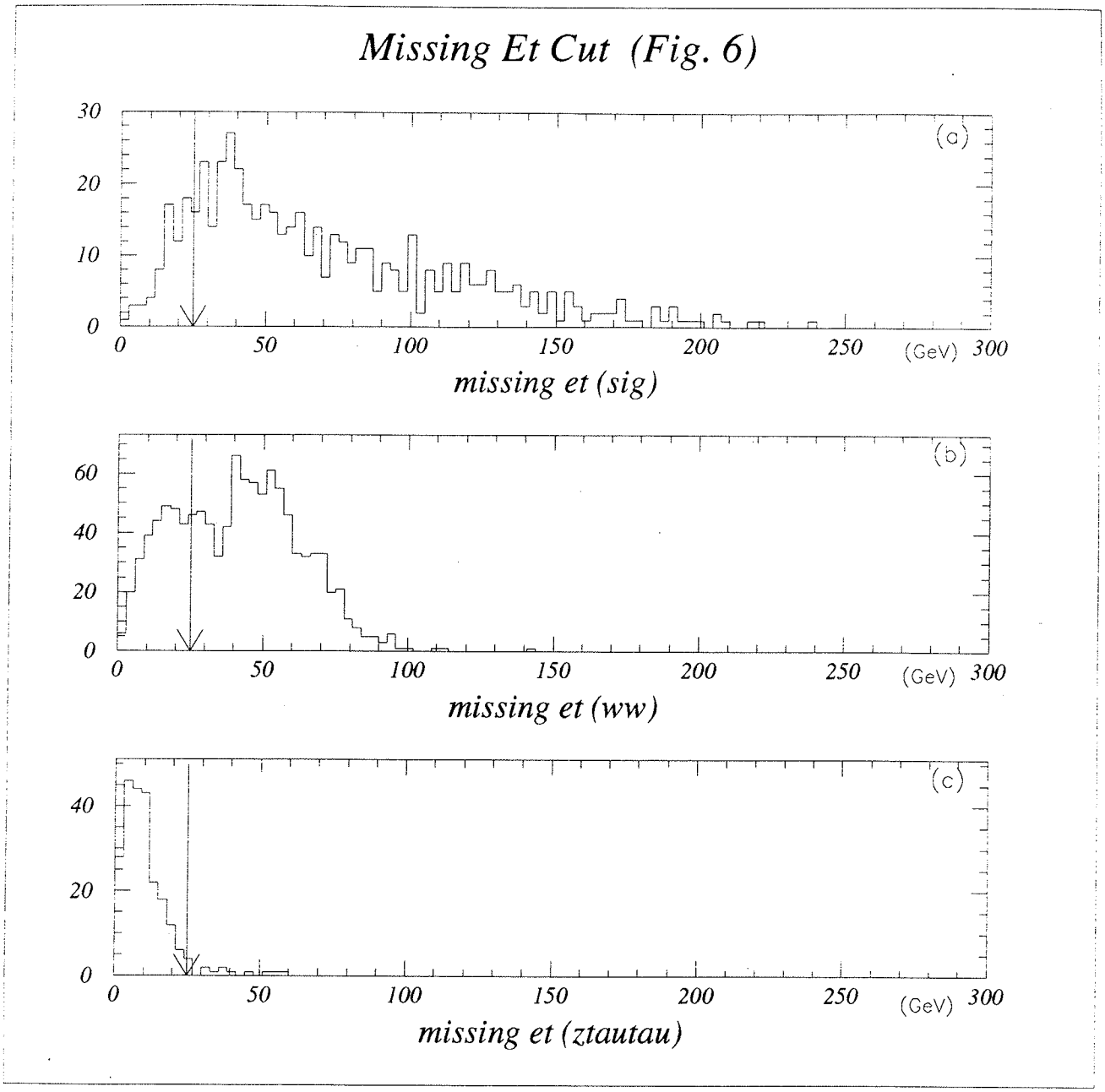
Missing Et Cut (Fig. 6)
30
20
10
0
0
50
100
150
200
250
(GeV)
300
(a)
missing et (sig)
60
40
20
0
(b)
missing et (ww)
40
20
0
(c)
missing et (ztautau)

FIG. 6.

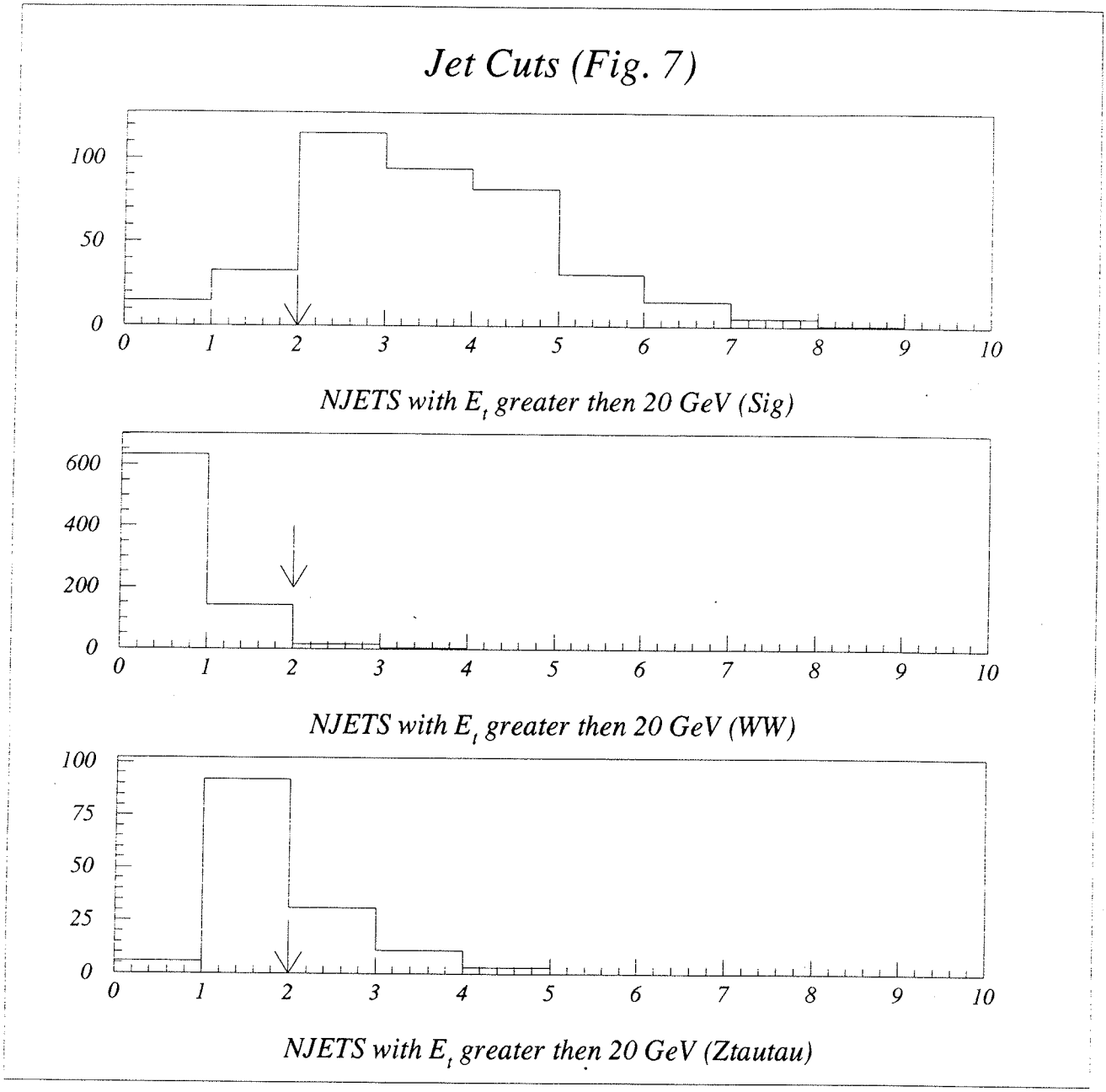
Jet Cuts (Fig. 7)
100
50
0
0 1 2 3 4 5 6 7 8 9 10
NJETS with E_t greater then 20 GeV (Sig)
600
400
200
0
0 1 2 3 4 5 6 7 8 9 10
NJETS with E_t greater then 20 GeV (WW)
100
75
50
25
0
0 1 2 3 4 5 6 7 8 9 10
NJETS with E_t greater then 20 GeV (Ztautau)

FIG. 7.

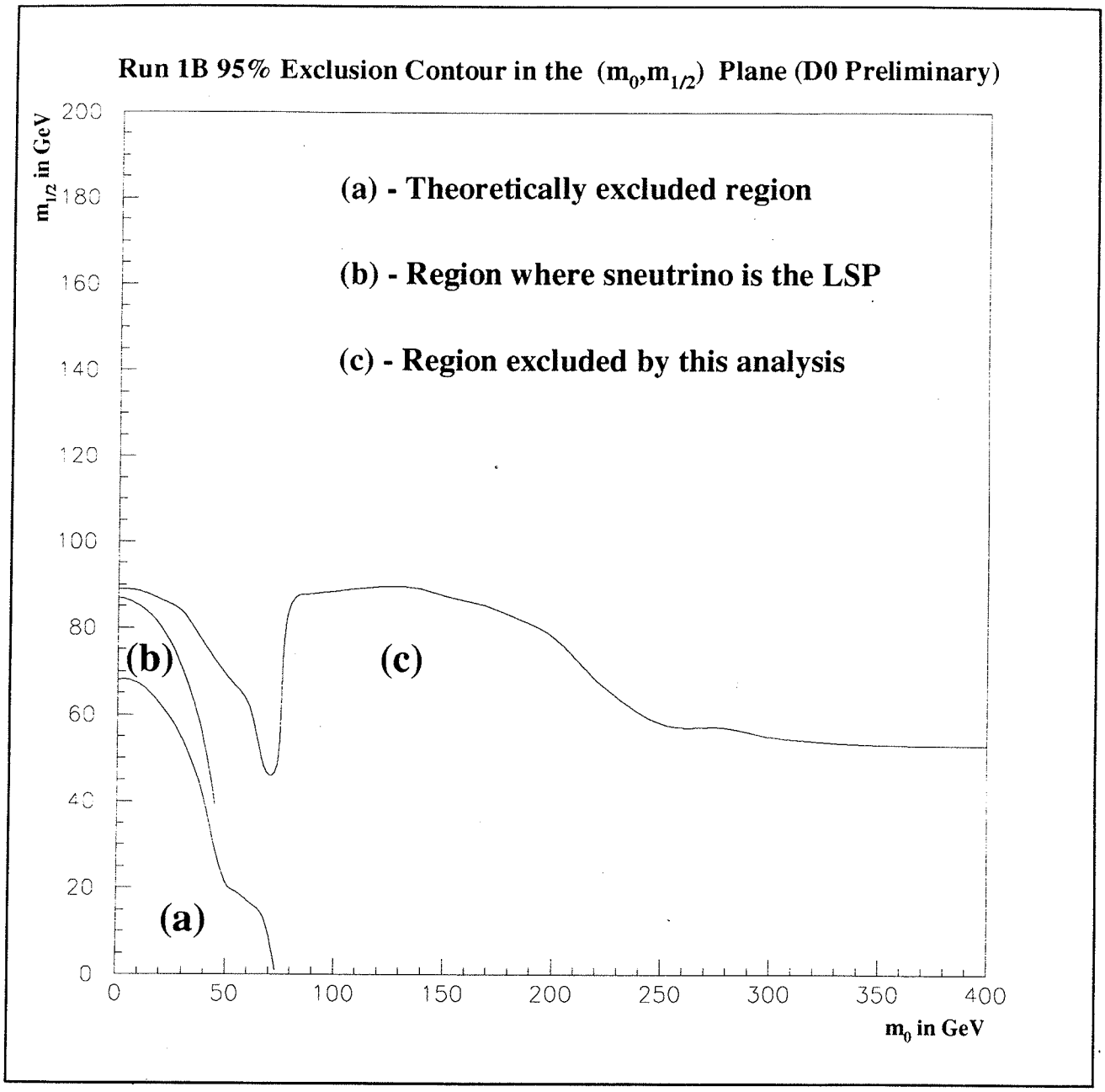

FIG. 8. 95% exclusion contour in the m_0-$m_{1/2}$ plane from the present analysis

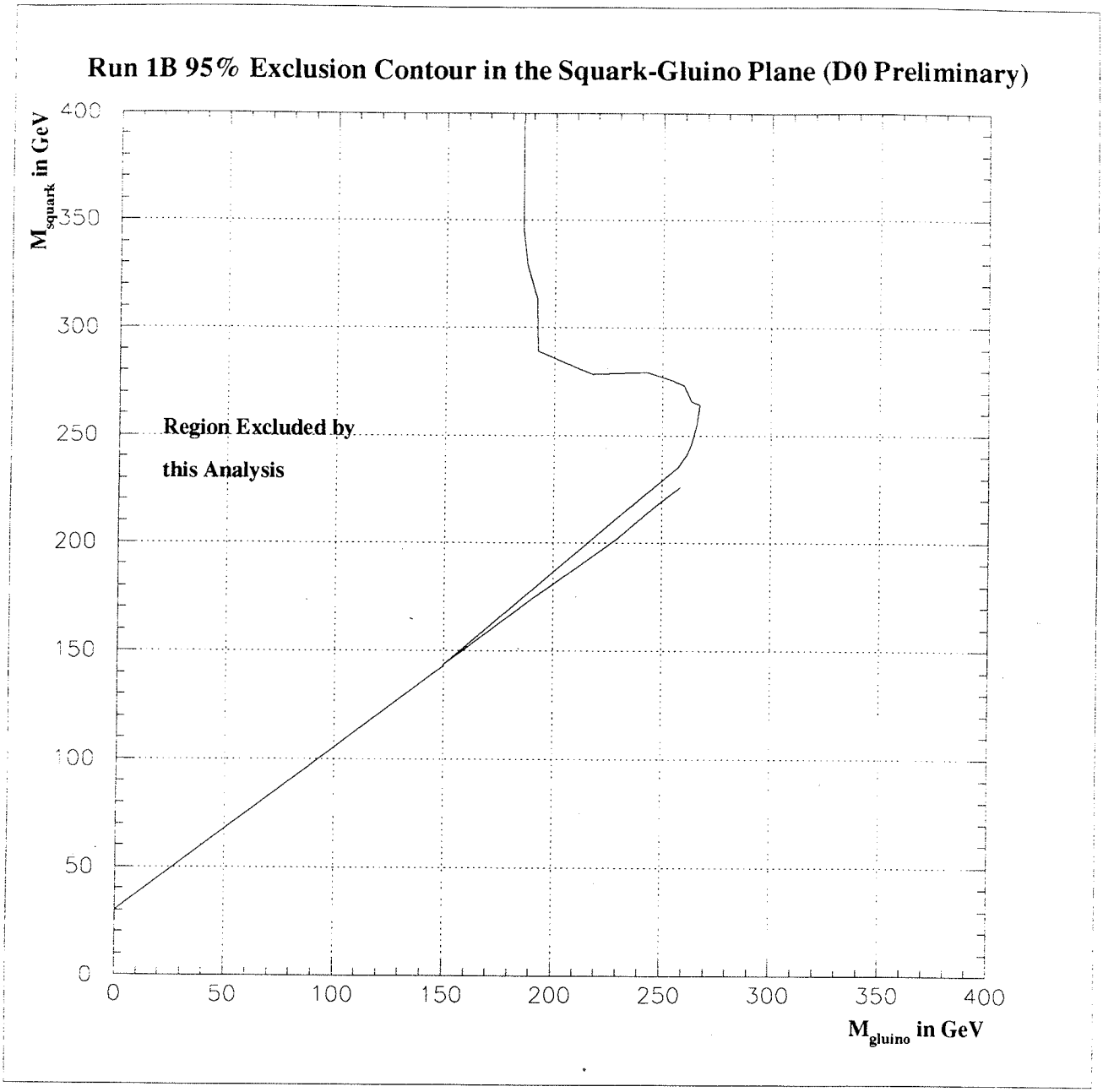

FIG. 9. 95 % exclusion contour in the squark-gluino plane from the present analysis